View metadata, citation and similar papers at core.ac.uk

brought to you by CORE

provided by Unitn-eprints Research

UNIVERSITY
OF TRENTO

DIPARTIMENTO DI INGEGNERIA E SCIENZA DELL'INFORMAZIONE

38123 Povo – Trento (Italy), Via Sommarive 14
http://www.disi.unitn.it

DETECTION OF BURIED INHOMOGENEOUS ELLIPTIC CYLINDERS BY A MEMETIC ALGORITHM

S. Caorsi, A. Massa, M. Pastorino, M. Raffetto, and A. Randazzo

January 2011

Technical Report # DISI-11-013

DETECTION OF BURIED INHOMOGENEOUS ELLIPTIC CYLINDERS BY A MEMETIC ALGORITHM

S. Caorsi[1], A. Massa[2], M. Pastorino[3], M. Raffetto[3], A. Randazzo[3]

1 Department of Electronics
University of Pavia
Via Ferrata 1
27100 Pavia, ITALY.
Phone: + 39 0382505661 Fax: +39 0382422583 e-mail: caorsi@ele.unipv.it

2 Department of Information and Communication Technology
University of Trento
Via Sommarive 14
I-38050 Trento, ITALY.
Phone: +39 0461882057 Fax: +39 0461881696 e-mail: andrea.massa@ing.unitn.it

3 Department of Biophysical and Electronic Engineering
University of Genoa
Via Opera Pia 11A
16145, Genova, ITALY.
Phone: +39 010 352242 Fax: +39 0103532245 e-mail: pastorino@dibe.unige.it

Abstract - The application of a global optimization procedure to the detection of buried inhomogeneities is studied in the present paper. The object inhomogeneities are schematized as multilayer infinite dielectric cylinders with elliptic cross sections. An efficient recursive analytical procedure is used for the forward scattering computation. A functional is constructed in which the field is expressed in series solution of Mathieu functions. Starting by the input scattered data, the iterative minimization of the functional is performed by a new optimization method called memetic algorithm.

Keywords: Electromagnetic imaging, elliptic cylinders, evolutionary algorithms

I. INTRODUCTION

The detection of buried inhomogeneities is a challenging topic in several applications, including nondestructive evaluation and testing, civil engineering, medical imaging, and subsurface diagnostics [1]-[8]. Recent efforts have been concentrated on solving the inverse scattering problem, which is the basic formulation for the electromagnetic imaging at frequencies such that the linear dimensions of the inhomogeneities are of the same magnitude order of the wavelength.

The detection of tunnels, pipes and other cylindrical structures has been recently addressed in [9][10] by using a schematic representation of these structures as infinite cylinders of cylindrical and elliptical cross sections and resorting to a numerical model in order to compute the forward scattering needed for the developed iterative procedure. In the present paper, we still consider the same elliptical geometry, but an efficient analytical solution is used for the forward scattering computation. Moreover, in order to take into account possible layered inhomogeneous structures, we let the elliptic cylinder to be multilayer and the retrieval of the dimensions and dielectric properties of the various layers is one of the aims of the proposed inverse procedure.

The other novelty of the paper concerns the applied optimization procedure. The inverse scattering problem is a highly nonlinear ill-posed problem [11]. Two approaches are usually followed to face this problem. The first one concerns the use of linearized procedures [12], which can allow for a quasi-real-time qualitative imaging, whereas the use of iterative procedures (computationally more heavy) allows the inspection of highly contrasted inhomogeneities. Among the iterative procedures, stochastic optimization algorithms are potentially able to obtain the global minimum of a given functional resulting from the formulation of the inverse scattering problem. The global solution coincides with the "true" solution, whose retrieval is of main importance in several areas (e.g., medical imaging).

Recently, evolutionary algorithms (in particular, the genetic algorithm [13]-[16]) have been widely proposed for solving optimization problems in inverse scattering [17]-[20]. Several different implementations of the genetic algorithm have been used, concerning both the coding of the unknown and the genetic operators. Actually, one of the main features of the genetic algorithm is the possibility of using specific implementations application-oriented. However, in the present paper we explore the use of a new version of an evolutionary algorithm, called memetic algorithm [21], which seems to be very suitable for the proposed application. In fact, the memetic algorithm, during the iterative evolution, considers only local minima of the cost function, so that a great speed-up is introduced in the search process. Moreover, since the algorithm population is composed

by only local optima, the number of individuals involved in the evolution can be chosen very little, even equal to the number of unknowns.

In the following, the mathematical formulation of the approach is presented, together with some numerical examples, which provide a preliminary assessment of the capabilities of the approach.

II. MATHEMATICAL FORMULATION

The assumed problem geometry is shown in Figure 1. A layered infinite cylinder, composed by *L* confocal elliptical layers, is positioned in a cross-borehole configuration [9]. The cylinder axis coincides with the *z* axis. A set of *S* electromagnetic sources, positioned at points (in the transverse plane) $\mathbf{x}_s$, *s = 1,…,S*, illuminates the objects. Each source generates an incident field, $\mathbf{E}_i^{inc}(\mathbf{r})$, *i=1,…,S*. The total electric field, $\mathbf{E}_i^{tot}(\mathbf{r})$, *i=1,…,S*, is measured by *M* sensors along a probing line in the transverse plane. Each layer of the cylinder is characterized by the dielectric permittivity ε_i and the semi-major axis a_i. The half focal distance is indicated by *d*. Under the hypotheses of deep inclusions [9], the line-source field-scattered data can be computed in terms of Mathieu functions, which are the eigenfunctions of the elliptic cylinder. In particular, the *z*-component of the electric field in the external medium satisfies the following Helmholtz equation, written in a standard elliptic coordinate system (*u,v,z*) [22]:

$$\frac{1}{d^2\left(\cosh^2(u)-\cos^2(v)\right)}\left(\frac{\partial^2 E_{scatt}}{\partial u^2}+\frac{\partial^2 E_{scatt}}{\partial v^2}\right)+\frac{\partial^2 E_{scatt}}{\partial z^2}+K_i E_{scatt}=0 \tag{1}$$

The solution of this equation can be expressed as [22]:

$$\begin{aligned} E_{scatt}(u,v) = &\sum_{m=0}^{+\infty} e_m^{L+1} Mc_m^{(4)}(q_{L+1},u)ce_m(q_{L+1},v)+ \\ &+\sum_{m=0}^{+\infty} o_m^{L+1} Ms_m^{(4)}(q_{L+1},u)se_m(q_{L+1},v) \end{aligned} \tag{2}$$

where q_{L+1} is given, for *i*=*L*+1, by

$$q_i=(k_i d/2)^2 \tag{3}$$

(being k_i the wavenumber of the i-th layer) and $Mc_{\mathrm{m}}^{(4)}$, $Ms_m^{(4)}$, ce_m and se_m are the fourth-order radial and angular Mathieu functions, respectively. Moreover, in equation (2), e_m^{L+1} and o_m^{L+1} are unknown coefficients to be determined. Analogously, in the generic i-th layer, the total electric field satisfies a Helmholtz equation similar to equation (1), whose solution is given by

$$\begin{aligned} E_z^i = &\sum_{m=0}^{+\infty}\left[e_{m,1}^i Mc_m^{(1)}(q_i,u)+e_{m,2}^i Mc_m^{(2)}(q_i,u)\right]ce_m(q_i,v)+ \\ &+\sum_{m=0}^{+\infty}\left[o_{m,1}^i Ms_m^{(1)}(q_i,u)+o_{m,2}^i Ms_m^{(2)}(q_i,u)\right]se_m(q_i,v) \end{aligned} \tag{4}$$

where $Mc_{\mathrm{m}}^{(1)}$, $Ms_m^{(2)}$, ce_m and se_m are odd and even radial Mathieu functions and $e^i_{m,1}$, $e^i_{m,2}$, $o^i_{m,1}$ and $o^i_{m,2}$ denote the unknown coefficients.

Finally, the known incident field can be expressed as:

$$E_z^{inc}(u,v)=\begin{cases} 2\pi\displaystyle\sum_{m=0}^{+\infty}\frac{Mc_m^{(4)}(q_{N+1},u_s)Mc_m^{(1)}(q_{N+1},u)ce_m(q_{N+1},v_s)ce_m(q_{N+1},v)}{\displaystyle\int_0^{2\pi}\left[ce_m(q_{N+1},v)\right]^2dv}+ \\ \displaystyle\sum_{m=0}^{+\infty}\frac{Ms_m^{(4)}(q_{N+1},u_s)Ms_m^{(1)}(q_{N+1},u)se_m(q_{N+1},v_s)se_m(q_{N+1},v)}{\displaystyle\int_0^{2\pi}\left[se_m(q_{N+1},v)\right]^2dv} & u<u_s \\ 2\pi\displaystyle\sum_{m=0}^{+\infty}\frac{Mc_m^{(4)}(q_{N+1},u)Mc_m^{(1)}(q_{N+1},u_s)ce_m(q_{N+1},v_s)ce_m(q_{N+1},v)}{\displaystyle\int_0^{2\pi}\left[ce_m(q_{N+1},v)\right]^2dv}+ \\ \displaystyle\sum_{m=0}^{+\infty}\frac{Ms_m^{(4)}(q_{N+1},u)Ms_m^{(1)}(q_{N+1},u_s)se_m(q_{N+1},v_s)se_m(q_{N+1},v)}{\displaystyle\int_0^{2\pi}\left[se_m(q_{N+1},v)\right]^2dv} & u>u_s \end{cases} \tag{5}$$

where u_s and v_s are the elliptic coordinates of the source. The corresponding magnetic field can be derived by the Maxwell equation in a straightforward way.

The unknown coefficients can be determined by truncating the above series (the Mathieu functions in different layers are not linearly independent sets) and applying the boundary conditions on the tangential components of $\mathbf{E}^{tot}(\mathbf{r})$ and $\mathbf{H}^{tot}(\mathbf{r})$ at all the dielectric boundaries:

$$\begin{cases} E_z^i(u_i,v) = E_z^{i+1}(u_i,v) & i=1,...,L-1 \\ E_z^L(u_L,v) = E_z^{inc}(u_L,v) + E_z^{scatt}(u_L,v) \\ H_v^i(u_i,v) = H_v^{i+1}(u_i,v) & i=1,...,L-1 \\ H_v^L(u_L,v) = H_v^{inc}(u_L,v) + H_v^{scatt}(u_L,v) \end{cases} \tag{6}$$

where $u = u_i$ is the boundary between the i-th and the (i+1)-th layers.

However, an efficient and fast recursive procedure for the computation of the above coefficients (starting from the external and the innermost layers) has been proposed in [23] and is used in the present work for solving the forward problem.

Furthermore, the inverse scattering problem is recast as an optimization problem by defining the following cost function:

$$J(\xi_k) = \frac{\sum_{s=1}^{S}\sum_{m=1}^{M}\left|E_{scatt}^{(k)}(\mathbf{x}_m,\mathbf{x}_s,\omega_q,\xi_k) - E_{scatt}^{meas}(\mathbf{x}_m,\mathbf{x}_s,\omega_q)\right|^2}{\sum_{s=1}^{S}\sum_{m=1}^{M}\left|E_{scatt}^{meas}(\mathbf{x}_m,\mathbf{x}_s,\omega_q)\right|^2} \tag{7}$$

where k indicates the iteration of the minimization algorithm and ξ_k is an array that contains the problem unknowns, which is given by

$$\xi_k = (x_0, y_0, a_1, ..., a_L, \varepsilon_1, ..., \varepsilon_L, d) \tag{8}$$

In order to minimize $J(\xi_k)$ and find (possibly) the global minimum, a so-called memetic algorithm is exploited.

It should be noticed that the above functional can be easily extended to multifrequency imaging.

III. MEMETIC ALGORITHMS

Memetic algorithms are optimization methods that belong to the family of evolutionary methods. In particular, they can be thought as hybrid genetic algorithms. The basic idea of the memetic algorithm is to emulate the idea transmission process. To this end, the new approach is based on the concept of meme [21]. A meme is a unit of information that can be transmitted when people exchange ideas. Memetic algorithms are population-based algorithms, in which every “idea”

is an individual. Since people process any idea to obtain a personal optimum before propagating it, each individual is a point of local minima of the cost function.

The evolution of the population is modeled by using the same operators of the genetic algorithm, i. e., selection, crossover and mutation. Since these operators are not generally able to produce local optima, an optimization procedure is needed.

The general schema of a memetic algorithm is shown in Figure 2. Let us consider a generic individual denoted by x_k:

$$x_k=(x_k^1,\ldots, x_k^m) \tag{9}$$

where x_k^i belongs to $\Re$ (real number set). The population of the algorithm is composed by N individuals:

$$P_i = \{x_k : k = 1,...,N\} \tag{10}$$

where the subscript "*i*" indicates the generation's number. An initial population P_0 is generated by randomly choosing N arrays in the search domain. Generally, these arrays are not points corresponding to local minima of the cost function; consequently, a local optimization procedure is applied to every vector x_k in order to obtain a point of minimum x_k^*. Such a procedure is denoted by $O(x_k)$ and is defined as:

$$O:\Re^m \ni x_k \to x_k^* \in \Re^m \tag{11}$$

where $\Re^m$ is the search space. The new individuals, called x_k^*, $k=1,\ldots,N$, generated by the optimization process, represent the new initial population P_0^* of the algorithm. The algorithm core is composed by three operations, i.e., selection, reproduction and mutation, which are applied sequentially.

The selection mechanism is applied to the population to select the individuals to mate. The used selection is the tournament selection [13], where the individuals are selected by randomly choosing (with uniform probability density) a subset of the current population. The reproduction mechanism adopted in this work is the proportional selection. Let x_1 and x_2 be two selected individuals. Reproduction generates a new individual x_3 such that:

$$x_3 = R(x_1, x_2) = ax_1 + (1-a)x_2 \tag{12}$$

where a is a random variable uniformly chosen in the interval (0,1). The mutation operator is the standard uniform mutation [13]. Let x_1 be the individual selected to mutate; the new individual x_2 is generated according to the following rule:

$$x_2 = M(x_1) = x_1 + \nu \tag{13}$$

where ν is an uniform random array chosen in the range of variation of the variables. The reproduction and mutation operators are executed with probabilities p_r and p_m, respectively. The applied recombination operators generate N_r and N_m new individuals, respectively, according to the reproduction and mutation probability. At the i-th iteration, a new population, called P_i', is generated by joining the old population P_i (that contains N individuals) and the N_r+N_m new individuals. Since P_i' contains more vectors than the N needed, it is necessary to reduce the population dimension. The individuals to propagate are chosen according to the following rule. The reproduced and mutated elements are always propagated. Moreover, if N_r+N_m is less than the population size N, the best individual and some randomly chosen arrays of the old generation are propagated.

The obtained population, called P_{i+1}, is composed by arrays that are not local minima and the local search procedure $O(x_i)$ is applied again. As a result, the new population of the memetic algorithm P_{i+1}^* is generated. Since the population is composed by only local minima, the individuals evolve over the search domain by "jumping" from a minimum to another one and a great speed up in the optimization procedure is obtained. Moreover, since the population is only composed by local minima, a reduced number of elements can be considered (e.g., equal to the number of uknown), with a significant computational saving.

IV. NUMERICAL RESULTS

Some preliminary results are reported in this section. With reference to the problem geometry shown in Figure 1, we consider a three-layer cylinder. The semi major axes of the ellipses are $0.3\lambda_b$, $0.39\lambda_b$, and $0.48\lambda_b$, being λ_b the wavelength of the incident radiation in the background medium, which is characterized by $\varepsilon_b = 12.0\varepsilon_0$ and $\mu_b = \mu_0$. The semi-focal distance is equal to $0.024\lambda_b$ and the cross-section center is at point $(0.3\lambda_b, -0.7\lambda_b)$.

The cylinder is illuminated by a single line source located, in the transversal plane at $\mathbf{x_s}$ = (0, $-0.7\lambda_b$). The total electric field is measured by a set of 21 sensors, uniformly distributed along a probing line in the borehole located at $x = 0.6\lambda_b$. The distance between two sensors is $0.06\lambda_b$.

First of all, a study of the cost function has been performed in order to evaluate the degree of nonlinearity. Results of this study are shown in Figure 3 and Figure 4. In particular, Figure 3 shows the behavior of the cost function when only the y coordinate of the cross-section center is changed, while Figure 4 shows the variations with respect to the permittivity value of the internal layer. As can be seen from these figures, the cost function exhibits some minima, both along the space direction related to the y coordinate of the cross-section center and along the one related to the dielectric permittivity. This behavior can justify the use of the proposed algorithm, which explores the search space only by jumping into the minima.

As a first test, the reconstruction of the dielectric cylinder is considered. The original relative dielectric permittivities of the three layers are equal to 12.0, 48.0 and 30.0, respectively. The crossover and mutation probabilities are p_r = 0.9 and p_m = 0.3 and the dimension of the population is chosen equal to the number of unknowns, whereas the maximum numbers of reproduced and mutated individuals are calculated according to the following rule:

$$\begin{aligned} N_r &= \lfloor N \cdot p_r \rfloor \\ N_m &= \lfloor (N - N_r) \cdot p_m + 1 \rfloor \end{aligned} \tag{14}$$

where $\lfloor x \rfloor$ indicates the biggest integer smaller than x.

The results are shown in Figures 5-7 and demonstrate that the algorithm reaches the correct solution after only 15 iterations. In particular, Figure 5 gives the reconstructed values of the dielectric permittivities of the various layers and Figure 6 shows the behavior of the fitness function versus the iteration number. As can be seen, the fitness function assumes only a limited set of values, corresponding to local minima. The proposed algorithm does not use the elitism [13]: this causes the presence of oscillations in the cost function, since the same minimum is repeatedly encountered. Finally, Figure 7 shows the reconstructed profile of the cylinder at some significant iterations. The above simulation has been performed starting from noiseless analytical data. The same computation has been repeated after corrupting the input data by adding random sequences corresponding to Gaussian noise with zero mean values and variances related to the fixed signal-to-noise ratios (SNRs). In the case in which SNR = 20 dB, a rather accurate reconstruction has been obtained after 20 iterations. In particular, the dielectric properties have been retrieved with minimum, mean, and maximum square errors equal to 0.0025, 0.092, and 0.24. The quality of the

data inversion becomes worst when the SNR is reduced to 10 dB. In this case, the same reconstruction errors are equal to 0.001, 0.12, and 0.36.

In another test, only the center of the cylinder is changed. The values of the relative dielectric permittivities used for this test are 24.0, 30.0 and 36.0, respectively. The other parameters are left unchanged. The obtained results are shown in Figures 8 and 9. In particular, Figure 8 shows the behavior of the retrieved cross-section center (x and y coordinates) versus the iteration number. Moreover, Figure 9 shows the cost function versus the iteration number. As can be seen from these figures, the convergence is reached in only three iterations, and after one iteration the candidate solution is already very close to the correct solution, even if the initial guess is very far from it.

Although the number of unknowns is small, a deterministic algorithm is not able to reach the exact solution as can be deduced from the results reported in Figures 10 and 11, which have been obtained by using a conjugate gradient (CG) procedure for comparison purposes. In particular, Figure 10 gives the plots of the functional J (equation (7)), calculated as follows:

$$J(t) = J\left(\xi_k + t\left(\xi_f - \xi_k\right)\right) \quad -0.5 \le t \le 1.5 \qquad k = 0, 1, 2, \ldots \tag{15}$$

where ξ_k denotes the current solution of the CG procedure and the starting point ξ_0 is assumed to be equal to the best starting point of the memetic algorithm; ξ_f indicates the point where the global minimum is located. It is evident that the deterministic procedure falls in a local minimum after only a few iterations. On the contrary, the MA-based inversion procedure is able to reach the exact solution as shown in Figure 11, where the same quantity is provided for different iteration values of the stochastic algorithm.

V. CONCLUSIONS

A new optimization method has been applied to the detection of multilayer infinite cylinders describing buried inhomogeneities. The optimization process is performed by a memetic algorithm, in which a series of local searches precede the global search performed by a genetic algorithm. At any iteration, the population is constituted by local minima. The approach has been found to be effective in dealing with the functional derived from the line-source inverse scattering problem for multilayer elliptic cylinders (which exhibits a number of local minima in all the directions of the search space). The obtained results, although preliminary, are rather interesting and indicate that a limited number of iterations is sufficient to obtain a correct localization of the multilayer elliptic

cylinder, for which the forward problem, at the various iterations, has been analytically solved by an efficient recursive procedure.

ACKNOWLEDGMENT

The authors wish to thank Dr. Johan Wettergreen for providing the subroutines for the computation of the Mathieu functions.

REFERENCES

[1] C. Dourthe, Ch. Pichot, J. Y. Dauvignac, and J. Cariou, "Inversion algorithm and measurement system for microwave tomography of buried object," Radio Sci., vol. 35, pp. 1097-1108, Sept.-Oct. 2000.

[2] Z. Q. Zhang and Q. H. Liu, "Two nonlinear inverse methods for electromagnetic induction measurements," IEEE Trans. Geosci. Remote Sensing, vol. 39, pp. 1331-1339, 2001.

[3] I. T. Rekanos and T. D. Tsiboukis, "A finite element-based technique for microwave imaging of two-dimensional objects," IEEE Trans. Instrum. Meas., vol. 49, pp. 234-239, 2000.

[4] S. J. Lockwood and H. Lee, "Pulse-echo microwave imaging for NDE of civil structures: Image reconstruction, enhancement, and object recognition," Int. J. Imaging Systems Technol., vol. 8, pp. 407-412, 1997.

[5] L. Chommeloux, Ch. Pichot, and J.-C. Bolomey, "Electromagnetic modeling for microwave imaging of cylindrical buried inhomogeneities," IEEE Trans. Microwave Theory Tech., vol. 34, pp. 1064-1076, Oct. 1986.

[6] S. Caorsi, G. L. Gragnani and M. Pastorino, "Numerical electromagnetic inverse-scattering solutions for two-dimensional infinite dielectric cylinders buried in a lossy half-space," IEEE Trans. Microwave Theory Tech., vol. 41, pp. 352-356, Feb. 1993.

[7] S. K. Moore, "Better breast cancer detection," IEEE Spectrum, May issue, pp. 50-55, 2001.

[8] D. Hughes and R. Zoughi, "A method for evaluating the dielectric properties of composites using a combined embedded modulated scattering and near-field microwave nondestructive testing technique," Proc. 18th IEEE Instrum. Meas. Techol. Conf., Budapest, Hungary, pp. 1882-1886, 2001.

[9] K. A. Michalski, Electromagnetic imaging of elliptical-cylindrical conductors and tunnels using a differential evolution algorithm, Microwave and Opt. Tecnol. Lett. 28 (2001) 164-167.

[10] K. A. Michalski, "A neural-network approach to the electromagnetic imaging of elliptic conducting cylinders," Microwave Opt. Tecnol. Lett., vol. 28, pp. 303-306, 2001.

[11] W. C. Chew and Y. M. Wang, "Reconstruction of two-dimensional permittivity dinstribution using the distorted Born iterative method," IEEE Trans. Med. Imaging, vol. 9, pp. 218-225, 1990.

[12] M. Slaney, A. C. Kak, and L. E. Larsen, "Limitation of imaging with first-order diffraction tomography," IEEE Trans. Microwave Theory Tech., vol. 32, pp. 860-873, 1984.

[13] D. Golberg, "Genetic and evolutionary algorithms come of age" *Comm. of the ACM,* vol. 37, pp. 113-119, 1994.

[14] R. L. Haupt, "An introduction to genetic algorithms for electromagnetics," IEEE Antennas Propagat. Magazine, 37, 2, 7-15, 1995.

[15] D. S. Weile and E. Michielssen, "Genetic algorithm optimization applied to electromagnetics: a review," IEEE Trans. Antennas Propagat, vol. 45, pp. 343-353, March 1997.

[16] J. M. Johnson and Y. Rahmat-Samii, "Genetic algorithms in engineering electromagnetics," IEEE Antennas Propagat. Mag., vol. 39, pp. 7-25, Apr. 1997.

[17] Z. P. Qian and W. Hong, "Image reconstruction of conducting cylinder based on FD-MEI and genetic algorithm," Proc. IEEE APS Int. Symp., vol. 2, pp. 718-721, 1998.

[18] C. C. Chiu and P. T. Liu, "Image reconstruction of a perfectly conducting cylinder by the genetic algorithm," IEE Proc. Microwave Antennas Propag., vol. 143, 1996.

[19] S. Caorsi, A. Massa, and M. Pastorino, "A microwave imaging procedure for NDT identification of a crack based on a genetic algorithm for nondestructive testing," IEEE Transactions on Antennas Propagat., vol. 49, no. 12, Dec. 2001.

[20] S. Kent and T. Gunel, "Dielectric permittivity estimation of cylindrical objects using genetic algorithm," J. Microwave Power and Electromagn. Energy, vol. 32, pp. 109-113, 1997.

[21] P. Moscato, “On evolution, search, optimization, genetic algorithms and martial arts towards memetic algorithms,” Tech. Rep. Caltech Concurrent Computation Program, Report. 826, California Institute of Technology, Pasadena, California, USA, 1989.

[22] J. J. Bowman, T. B. A. Senior, and P. L. E. Uslenghi, Electromagnetic and Acoustic Scattering by Simple Shapes. Amsterdam, The Netherlands: North-Holland, 1969.

[23] S. Caorsi, M. Pastorino and M. Raffetto, "Electromagnetic scattering by a multilayer elliptic cylinder: series solution in terms of Mathieu functions," IEEE Trans. Antennas Propagat., vol. 45, pp. 926-935, June 1997.

FIGURE CAPTIONS

Figure 1 – Geometrical configuration.

Figure 2 – Memetic algorithm flow chart.

Figure 3 – Fitness function versus y coordinate of the cross-section center.

Figure 4 – Fitness function versus the dielectric permittivity of the first layer (normalized to the background permittivity).

Figure 5 – Values of the normalized dielectric permittivities in the three layers of the elliptic cylinder versus the iteration number.

Figure 6 – Fitness function versus the iteration number.

Figure 7 – Reconstructed normalized dielectric permittivities ($\varepsilon/\varepsilon_b$) in the three layers of the elliptic cylinder ($y = -0.7\lambda_b$).

Figure 8 – Localization of the cross-section center (x and y coordinates) versus the iteration number

Figure 9 – Fitness function versus the iteration number.

Figure 10 - Behavior of the fitness function (equation (15)) plotted along a straight line connecting the current solution (at the k_{CG}-th iteration) and the exact solution, for different values of the iteration number of the conjugate gradient procedure.

Figure 11 - Behavior of the fitness function (equation (15)) plotted along a straight line connecting the current solution (at the k_{MA}-th iteration) and the exact solution, for different values of the iteration number of the memetic algorithm.

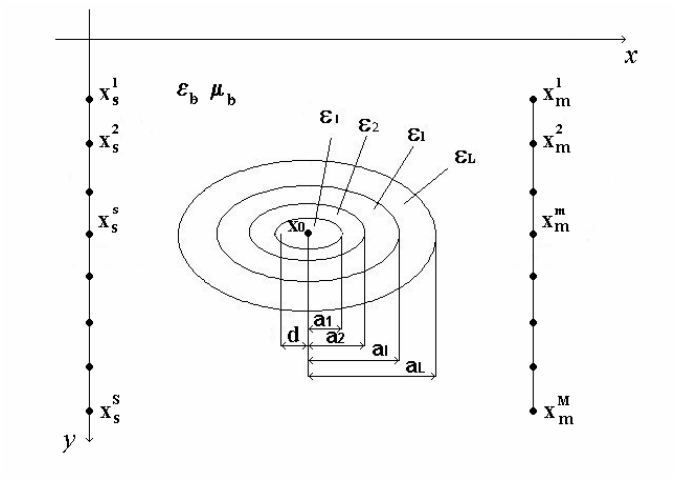
x
y
ε_b μ_b
ε_1
ε_2
ε_l
ε_L
x_0
d
a_1
a_2
a_l
a_L
x_s^1
x_s^2
x_s^s
x_s^S
x_m^1
x_m^2
x_m^m
x_m^M

Figure 1

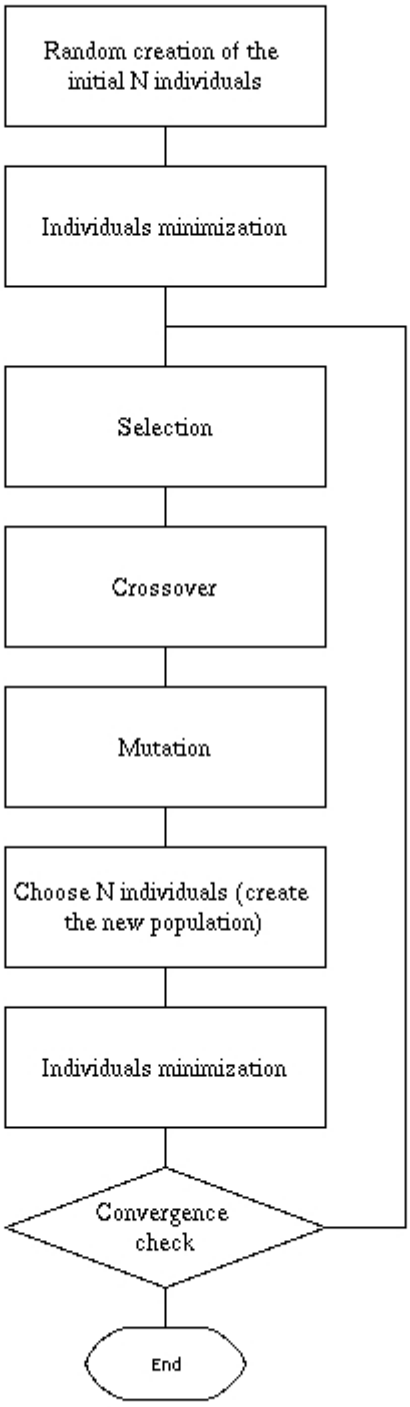
Random creation of the initial N individuals
Individuals minimization
Selection
Crossover
Mutation
Choose N individuals (create the new population)
Individuals minimization
Convergence check
End

Figure 2

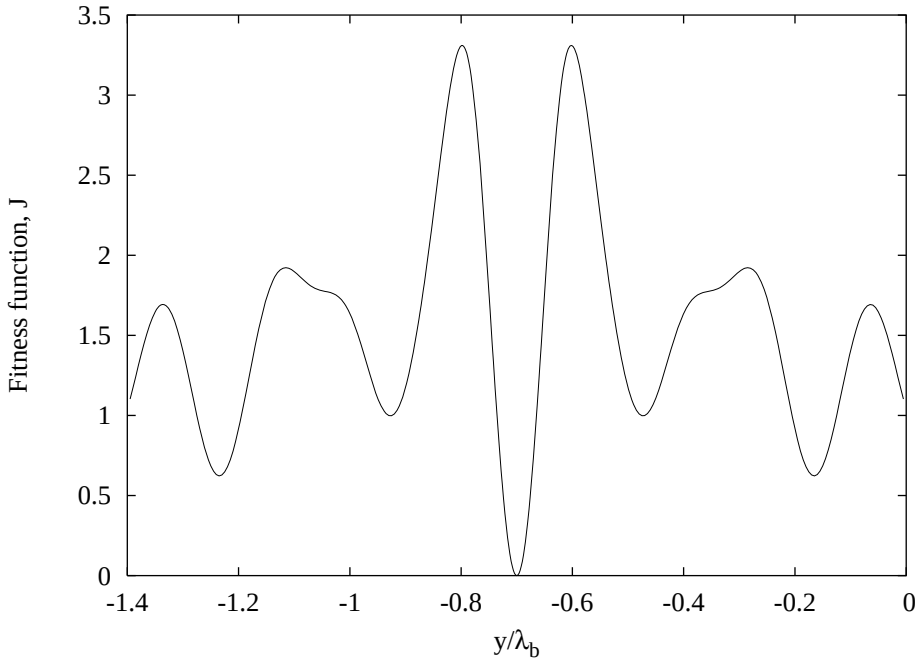

Figure 3

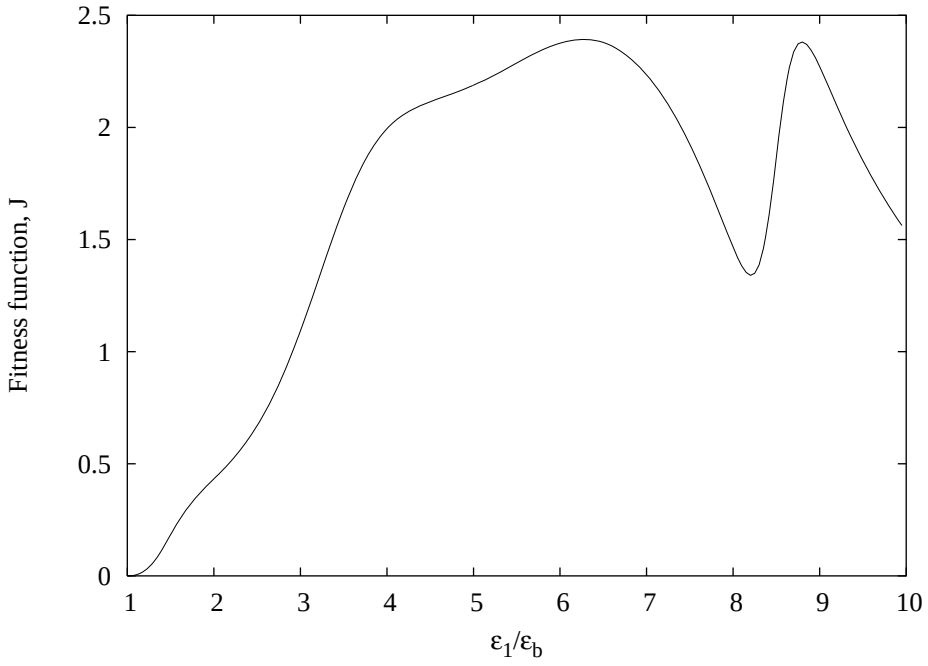

Figure 4

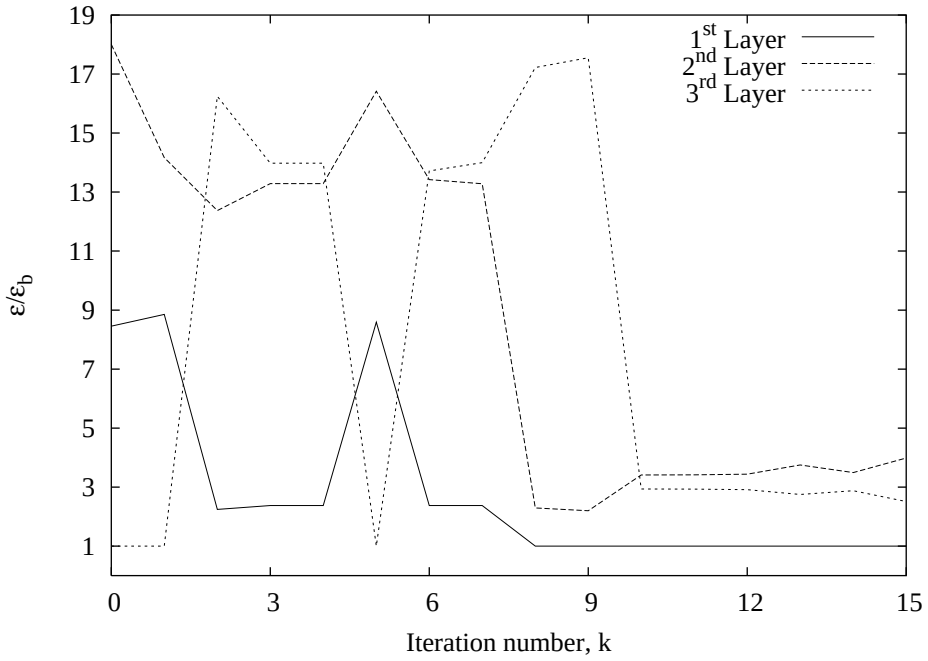

Figure 5

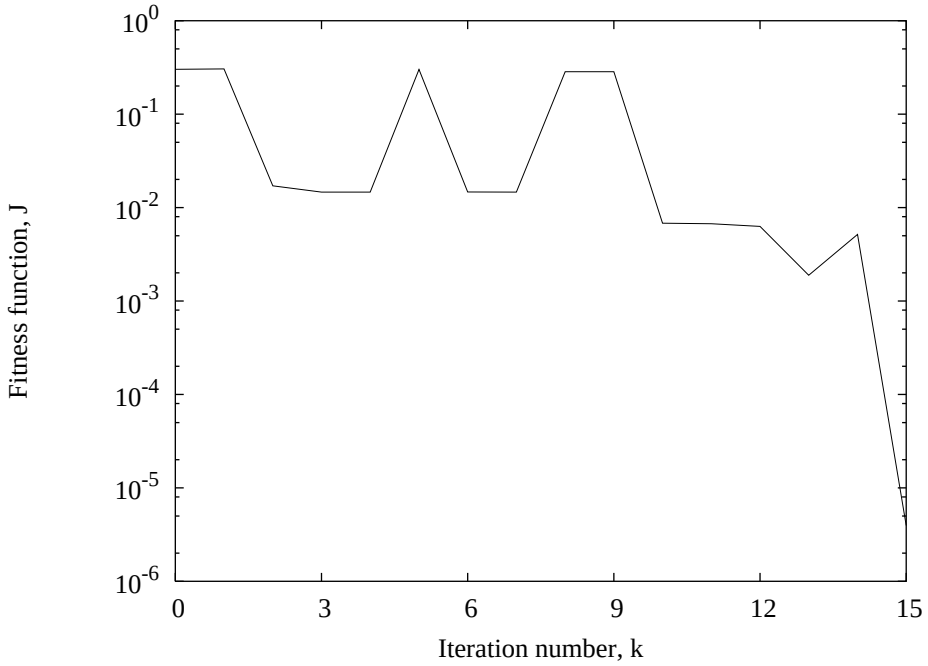

Figure 6

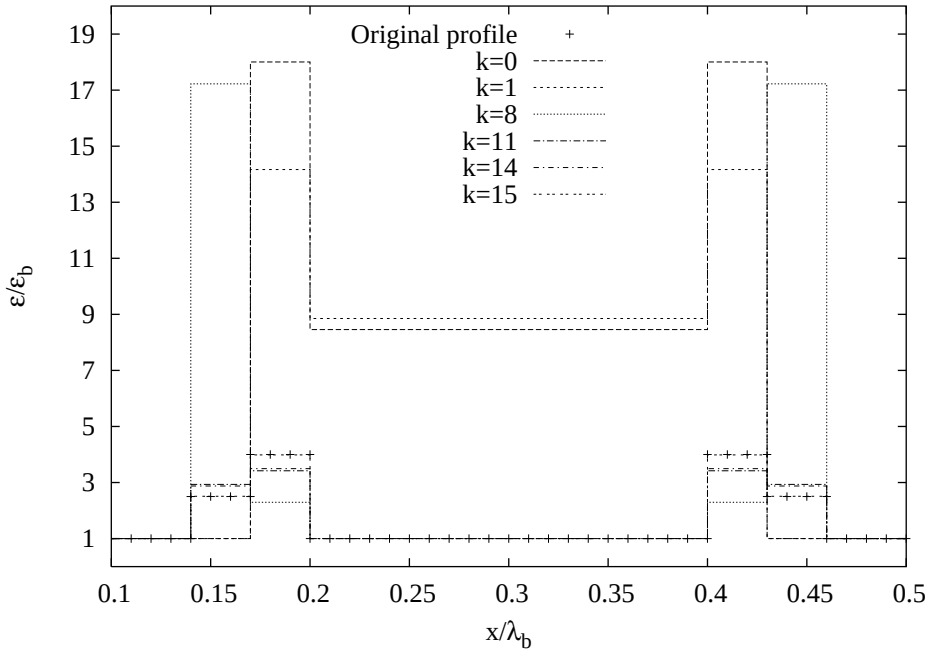

Figure 7

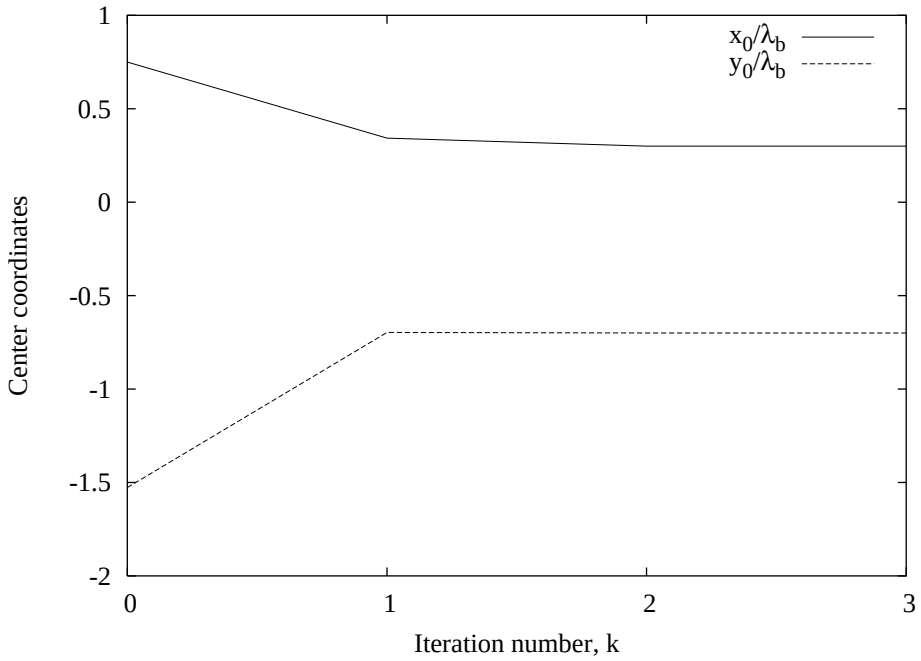

Figure 8

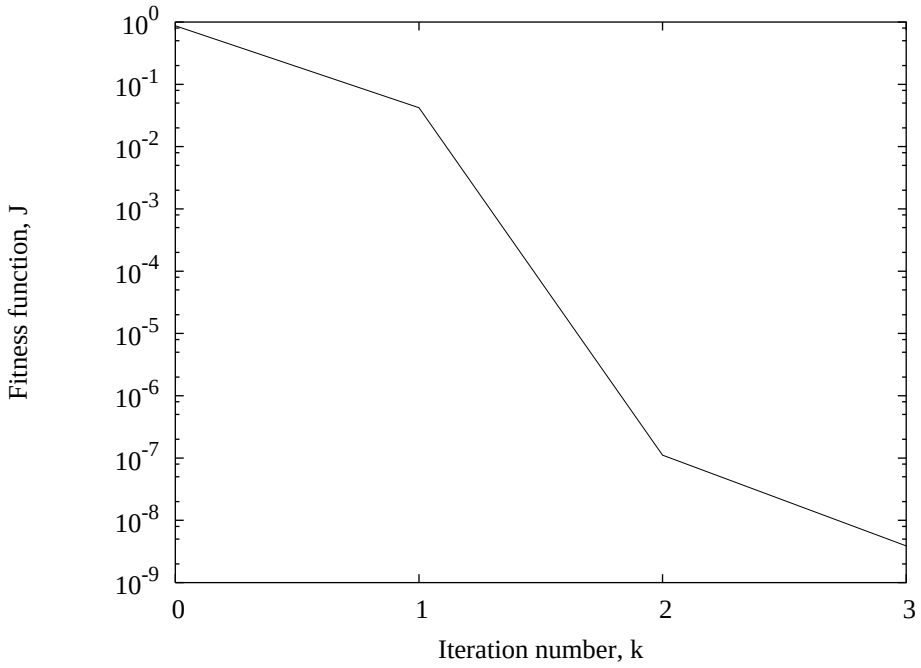

Figure 9

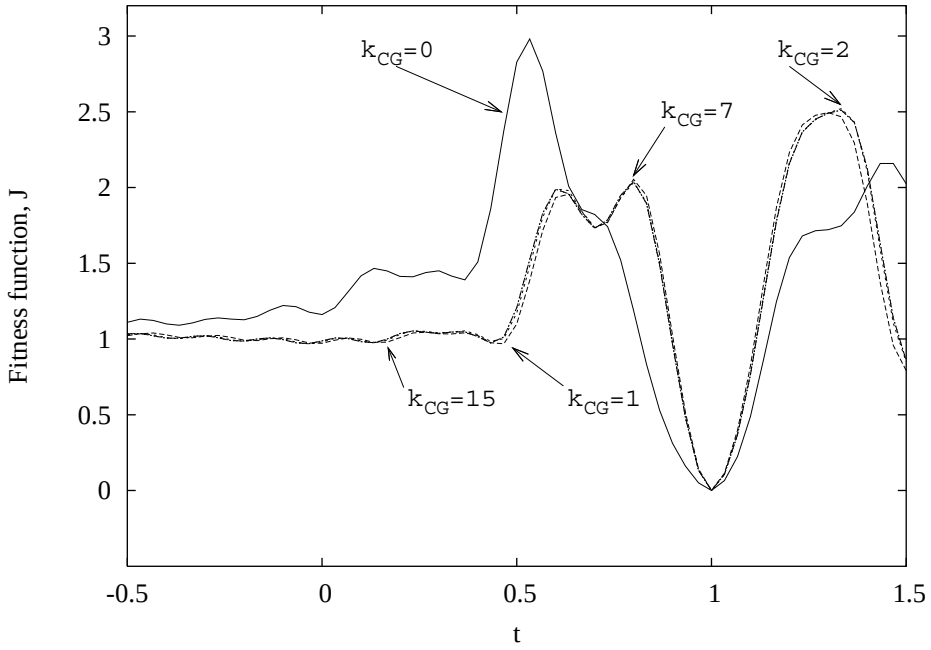

Figure 10

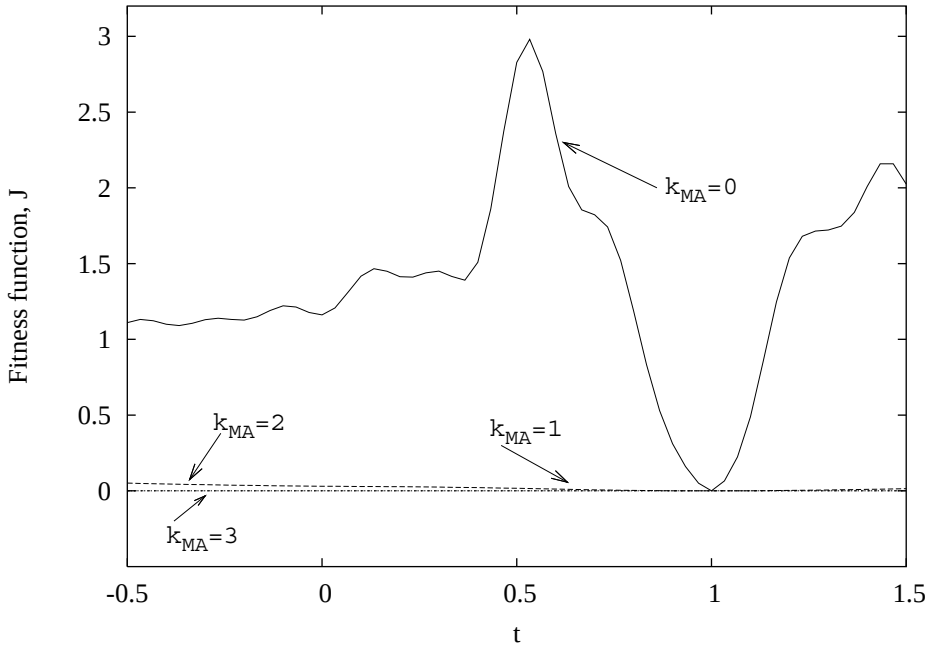
Fitness function, J
t
3
2.5
2
1.5
1
0.5
0
-0.5
0
0.5
1
1.5
k_MA=0
k_MA=1
k_MA=2
k_MA=3

Figure 11